

# Predicting Wheelchair Stability while Crossing a Curb using RGB-Depth Vision

Aryan Naveen, Haitao Luo, Zhimin Chen, and Bing Li\*

Clemson University, Department of Automotive Engineering  
4 Research Dr., Greenville, SC 29607, USA [bli4@clemson.edu](mailto:bli4@clemson.edu)

**Abstract.** Handicapped individuals often rely heavily on various assistive technologies including wheelchairs and the purpose of these technologies is to enable greater levels of independence for the user. In the development of autonomous wheelchairs, it is imperative that the wheelchair maintains appropriate stability for the user in an outdoor urban environment. This paper proposes an RGB-Depth based perception algorithm for 3D mapping of the environment in addition to dynamic modeling of the wheelchair for stability analysis and prediction. We utilize RTAB Mapping in combination with Poisson Reconstruction that produced triangular mesh from which an accurate prediction of the stability of the wheelchair can be made based on the normals and the critical angle calculated from the dynamic model of the wheelchair.

**Keywords:** Wheelchair Stability · Dynamics Model · Computer Vision · SLAM · Mesh Generation · 3D Reconstruction

## 1 Introduction

Individuals with cognitive, motor or sensory impairment, whether it is due to disability or disease, often rely heavily on wheelchairs. As of 2015, there were 2.7 million wheelchair users in the United States[3]. Autonomous wheelchairs have the ability to enable a higher level of independence for handicapped individuals, however the margin for error is small. Maintaining wheelchair stability goes a long way in preventing injuries to the user. This requirement-while traversing a dynamic outdoor urban environment- is extremely important and there are a wide array of terrains that an autonomous wheelchair must handle and ensure stability for the user.

In addition to avoiding obstacles, the terrain in many scenarios can pose hazards as they can cause orientations of a wheelchair that results in rollover. Essentially, in order to effectively accomplish this task of ensuring stability for the wheelchair the system must have a high level understanding of the surrounding terrain. Of course this presents numerous challenges that must be accounted for in order to develop a robust solution for stability prediction of an autonomous wheelchair. The first main challenge is understanding and mapping the environment accurately despite high levels of data noise. Multiple research works have

focused on building different 3D maps of a given environment with different information for the wheelchair. Murakara et. al analyzed the integration of vision and laser range finders to construct a 2 dimensional indoor safety map for a wheelchair [5]. Furthermore, Zhao et. al implemented a graph based SLAM approach for building a grid point cloud semantic map for indoor navigation of an autonomous wheelchair [7].

Another challenge is understanding the environment-wheelchair interaction. The parameters of the terrain needed for an unstable configuration (coefficient of friction and gradient) must be determined in terms of wheelchair parameters. In addition, modeling has been performed to account for various types of suspensions, chassises, and drive systems [4] [6]. In our case we treat the wheelchair as a rigid body and do not need to account for these factors as wheelchairs use simple differential drive without any suspension thereby simplifying the model. Furthermore, specific to wheelchairs, Candiotti et. al perform stability analysis with their novel electric power wheelchair, MEBot, based on analyzing the movement of the center of mass of the wheelchair [2].

This paper proposes an RGB-Depth based perception algorithm for 3D mapping of the environment in addition to dynamic modeling of the wheelchair for stability analysis and prediction. We employ RTAB mapping- based on graph SLAM- to construct a three dimensional pointcloud of the terrain and then convert the pointcloud to triangular mesh using Poisson Reconstruction. We then use the normals from the triangular mesh along with the dynamic model of the wheelchair to predict the stability of the wheelchair.

## 2 Curb Mapping

### 2.1 3D Mapping and Pointcloud Generation

To solve the problem of building a 3D map of the "safety zone" we employed RTAB which uses graph based SLAM algorithm to construct a pointcloud as shown in Figure 1. In graph based SLAM, the idea is to arrange the collected data in the form of a graph consisting of nodes and links. A node in the graph contains the pose of the sensor ,  $x_i$ , and the raw data,  $D$ , at a specific time step  $t$ , while a link contains the measurement constraints  $w_t$  and  $v_t$ . The Maximum Likelihood Principle (MLE) is used to then optimize the graph. We implemented this algorithm through a ROS package with an IntelRealsense D435i stereo camera.

### 2.2 3D Mesh Generation

The goal of mesh generation is to ensure that the mesh conform to the geometric characteristics of the generated pointcloud. We decided to employ Poisson Surface Reconstruction [1], proposed by Kazhdan et. al, because it highly resilient to data noise which will surely be encountered in a generated 3D map from an outdoor environment.

The problem of computing the indicator function boils down to finding the scalar function  $X$ , indicator function, whose gradient best approximates a vector field  $V$  defined by the sample  $S$ . Given a solid  $M$ , whose boundaries is  $\Gamma_M$ , and a smoothing filter  $F(q)$ , where  $F_p(q) = F(q - p)$ , a vector field  $\vec{V}(q)$  can be derived based on the input pointcloud  $S$ .

$$\vec{V}(q) = \sum_{s \in S} |\zeta_s| F_{s,p}(q) s.N \quad (1)$$

Then the indicator function,  $X$ , can be found by applying the divergence operator to  $V$  because  $X$  laplacian is equal to the divergence of  $V$ .

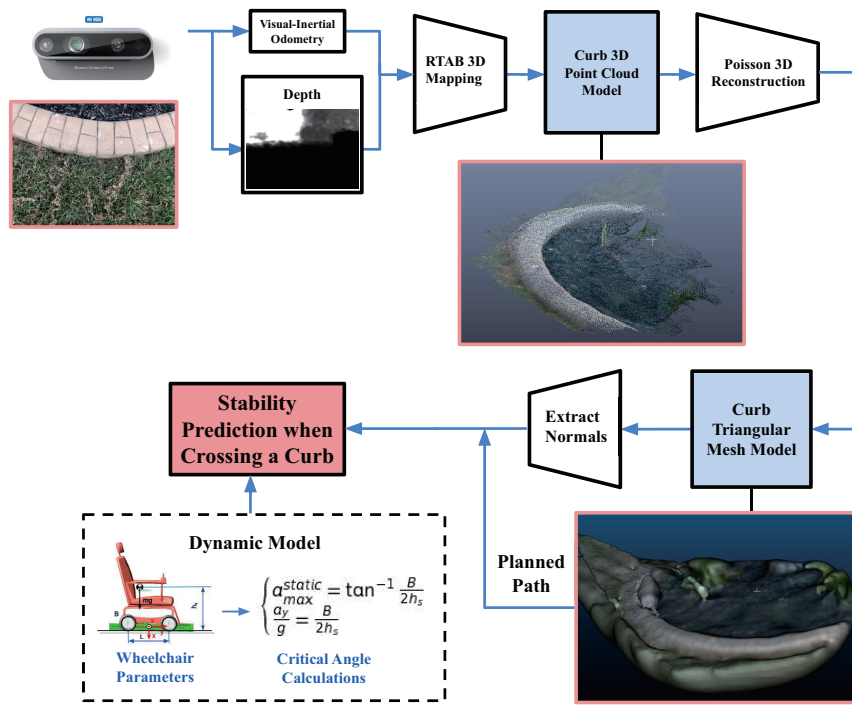


Fig. 1: 3D Mapping and Stability Prediction Pipeline

### 3 Dynamic Model of the Wheelchair Rollover Stability

The modeling process is based on the following assumptions: (1) the whole wheelchair is equivalent to rigid body, (2) the wheelchair is symmetrical with the middle plane of the wheels on both sides, and the center of mass lies on the middle plane, (3) the four-wheeled wheelchair model is equivalent to a two-wheeled model, where the two wheels in contact with the ground are equivalent to a longitudinal middle position, and the center of mass is located on this plane.

Figure 2 is a diagram of the wheelchair's static roll dynamics model. The following relationships between the forces at points A and C are given:  $F_i + F_o = mg \cos(\alpha)$  and  $F_{si} + F_{so} = mg \sin(\alpha)$ . Using these relations, the net force on the inner tire,  $F_1$ , and on the outer tire,  $F_2$ , can be derived in relation to the wheelchair parameters,  $h_s$  and  $B$ , by simply applying the lever rule.

$$\begin{cases} F_1 = (1 - \frac{B + (h_s \tan(\alpha) + \frac{B}{2})}{B})mg \\ F_2 = \frac{B - (h_s \tan(\alpha) + \frac{B}{2})}{B}mg \end{cases} \quad (2)$$

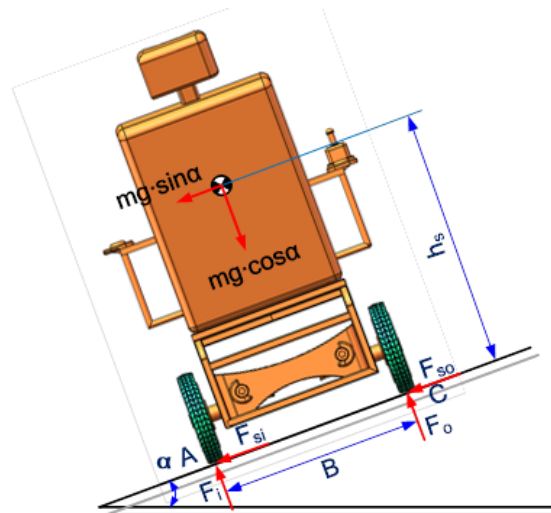


Fig. 2: Static model of wheelchair static rollover

Using the derived net forces for each tire, the conditions required for rollover in both a static and dynamic state can be calculated. In both situations when the wheelchair is at the critical rollover angle, the net force of the outer tire is 0. This condition is used to evaluate the maximum roll angle,  $\alpha_{max}^{static}$ , and

wheelchair dynamic rollover threshold,  $\frac{a_y}{g}$ .

$$\begin{cases} a_{max}^{static} = \tan^{-1} \frac{B}{2h_s} \\ \frac{a_y}{g} = \frac{B}{2h_s} \end{cases} \quad (3)$$

The above relations are used to evaluate the wheelchair's anti rollover capability.

## 4 Experiment

For the data collection using the IntelRealsense D435i, we implemented the SLAM based 3D mapping approach outlined above to construct maps of various curb terrains. The maps generally consisted of 2 meters of road or flat elevation followed by some obstacle, approximately 1 meter wide, and then another terrain such as grass or a ramp for another 2 meters to provide sufficient area for simulation purposes. The maps were constructed on an intel core i7, running ROS kinetic on Ubuntu 16.04. Visualization of the produced meshes from the proposed pipeline compared to the RGB image of the obstacle can be seen in Figure 3.

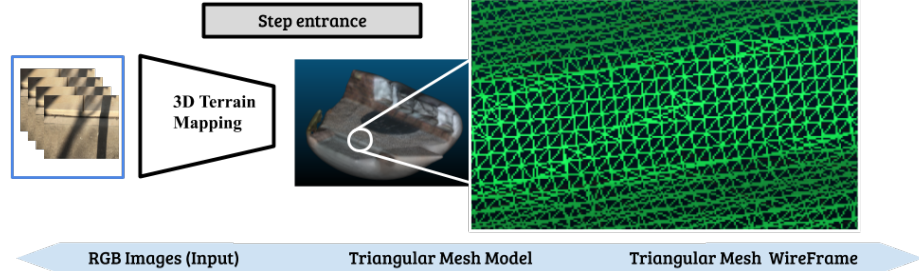


Fig. 3: Field collected data and mesh Generation Visualization Results

### 4.1 3D Mapping and Mesh Result

From both the gathered 3D pointcloud data as well as the cropped 3D pointcloud data the same mesh generation algorithm was run to produce the isosurface from the indicator function,  $X$ . The results proved that Poisson reconstruction produced mesh representations that were an effective representation for the 3D map while keeping the geometric characteristics of the data (Figure 1). The mesh quality metric used to assess the various meshing algorithms is Edge Root Mean Square (ERMS) as  $ERMS_\mu = \frac{1}{N} \sum_{t \in \Lambda_T} \sqrt{\frac{t_{L1}^2 + t_{L2}^2 + t_{L3}^2}{3}}$  where  $\Lambda_T$  is the set of

Table 1: Performance of mesh generation algorithms

| Edge Root Mean Square                     |         |                |          |         |
|---|---------|----------------|----------|---------|
| K   | 0.5     | 0.7            | 0.9      | 0.97    |
| Poisson Reconstruction — $O(m^3 \log(m))$ |         |                |          |         |
| $\mu$                                     | 0.00665 | <b>0.00478</b> | 0.00413  | 0.00429 |
| Alpha Shapes — $O(m^2)$                   |         |                |          |         |
| $\mu$                                     | 0.01596 | 0.01398        | 0.01268  | 0.01232 |
| Delaunay Triangulation — $O(m \log(m))$   |         |                |          |         |
| $\mu$                                     | 0.02621 | 0.02498        | 0.024193 | 0.02394 |

all triangles that make up the different meshes, and  $t_{L1}, t_{L2}, t_{L3}$ , are the legs of triangle  $t \in \Lambda_t$ . N is also the number of triangles in a given mesh.

Table 1 shows that the most optimal configuration for the mesh generation is Poisson Reconstruction after a subsample of  $K = 0.7$ , because Poisson Reconstruction's time complexity is polynomial. Furthermore, the extremely low ERMS for Poisson compared to the other methods demonstrates that the normal vectors calculated from the triangular mesh will be more accurate which enables better stability prediction.

#### 4.2 Dynamic Simulation on Field Collected Data

Establish the dynamic model of the wheelchair in ADAMS as seen in Figure 4. Among the parameters of the wheelchair, the three-dimensional size of the wheelchair (length x width x height) is 1000x710mmx1320mm, the wheelbase B is 650mm, the wheelbase L is 575mm, and the wheelchair's distance to the mass centroid from the ground  $h_s$  is 451mm. Taking into account the user's weight in the dynamic model of the wheelchair, the mass of the system now includes both the wheelchair's mass(65 kg) and the mass of the user (100kg), producing a total mass ( $m$ ) of 165kg. The four tire specifications of the wheelchair are 205/55 R16, this tire model uses magic formulas and is suitable for wheelchair roll stability analysis. Import field collected terrain data as ".rdf" file into ADAMS to generate 3D road simulation model as seen in Figure 4.

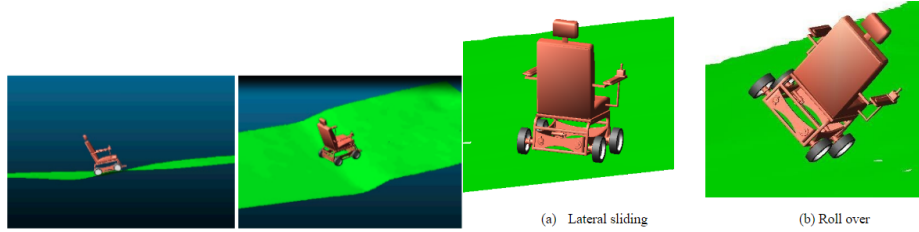


Fig. 4: Wheelchairs simulation in ADAMS on field collected data

The variations in both the acceleration as well as the posture angle as shown in Figure 5 demonstrate the anti-tipping characteristic of the wheelchair in the simulated environment. Both charts have similar trends in the sense that while driving over the initial flat road the values were relatively steady compared to the fluctuations caused by traversing the curb as well as the rugged terrain behind the curb.

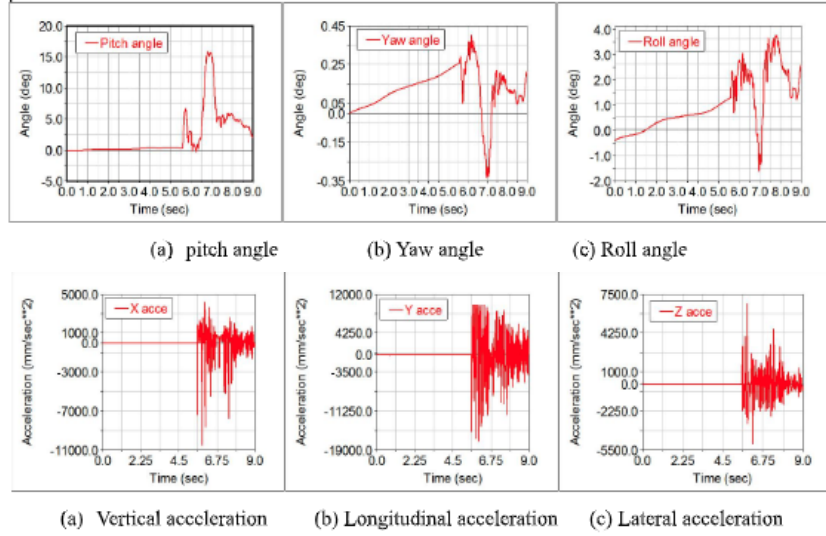


Fig. 5: Wheelchairs simulation in ADAMS on field collected data

Figure 4 also shows two kinds of unstable status of wheelchair when simulated in ADAMS, Figure 4 (a) is the lateral sliding statue and Figure 4 (b) is the rollover status. From Table 2, the critical rollover angle increases with increasing terrain coefficient of friction. When the terrain friction coefficient is less than 0.6, the unstable state of the wheelchair is represented by lateral sliding, otherwise it is rollover. In addition, the terrain rollover angle of 25 degrees is the dividing line between roll and sliding, and the friction coefficient of the corresponding terrain is 0.6. When the coefficient of terrain friction is greater than 0.6, the roll angle of the wheelchair fluctuates around 25 degrees with little change.

## 5 Conclusion

In this paper we have proposed a robust pipeline for 3D mapping of terrain for autonomous wheelchairs. In addition, we also developed a dynamic model for a wheelchair to be used for stability analysis and prediction. We utilize RTAB Mapping in combination with Poisson Reconstruction to produce triangular mesh (Figure 3) from which normals can be extracted to enable stability

Table 2: Wheelchair critical rollover stability w.r.t. terrain friction coefficients

| No. | Coefficient of friction of terrain | Critical Rollover angle ( $^{\circ}$ ) | Unstable state |
|-----|------------------------------------|--|----------------|
| 1   | 0.2                                | 8.2                                    | Sliding        |
| 2   | 0.4                                | 18.2                                   | Sliding        |
| 3   | 0.6                                | 22.8                                   | Sliding        |
| 4   | 0.8                                | 25.2                                   | Rollover       |
| 5   | 1.0                                | 25.8                                   | Rollover       |
| 6   | 1.2                                | 26.2                                   | Rollover       |
| 7   | 1.4                                | 26.5                                   | Rollover       |

predictions. An area of improvement in our work is the time complexity of the mesh generation algorithm. Although, poisson reconstruction was selected due to it's distinct characteristic of being resistant to data noise, it presents a poor time complexity that in this paper was dealt with by simply subsampling the 3D pointcloud. Also another interesting area to investigate is the influence of other terramechanical properties of terrain on stability of wheelchairs. In the future, the big picture plan for this work is to be integrated into a comprehensive autonomous wheelchair to help enable greater independence/mobility for a population that is handicapped.

## References

1. Matthew Bolitho, Michael Kazhdan, Randal Burns, and Hugues Hoppe. Parallel poisson surface reconstruction. *Advances in Visual Computing Lecture Notes in Computer Science*, page 678–689, 2009.
2. Jorge Candiotti, S. Andrea Sundaram, Brandon Daveler, Benjamin Gebrosky, Garrett Grindle, Hongwu Wang, and Rory A. Cooper. Kinematics and stability analysis of a novel power wheelchair when traversing architectural barriers. *Topics in Spinal Cord Injury Rehabilitation*, 23(2):110–119, 2017.
3. Alicia M et al. Koontz. Wheeled mobility. *BioMed research international*, 2015.
4. M. Levesley, S. Kember, David Barton, P. Brooks, and Osvaldo Querin. Dynamic simulation of vehicle suspension systems for durability analysis. *Materials Science Forum - MATER SCI FORUM*, 440-441:103–110, 01 2003.
5. A. Murarka, J. Modayil, and B. Kuipers. Building local safety maps for a wheelchair robot using vision and lasers. *The 3rd Canadian Conference on Computer and Robot Vision (CRV06)*.
6. Brad Schofield, Tore Hagglund, and Anders Rantzer. Vehicle dynamics control and controller allocation for rollover prevention. *2006 IEEE International Conference on Control Applications*, 2006.
7. Cheng Zhao, Huosheng Hu, and Dongbing Gu. Building a grid-point cloud-semantic map based on graph for the navigation of intelligent wheelchair. *2015 21st International Conference on Automation and Computing (ICAC)*, 2015.





---

# Predicting Wheelchair Stability while Crossing a curb using RGB-Depth Vision

Aryan Naveen, Haitao Luo, Zhimin Chen, and Bing Li

9 Sep 2020



## Problem Statement/Motivation

---

- Individuals with cognitive/motor/sensory impairment, whether it is due to disability or disease, often rely heavily on wheelchairs.
- Maintaining wheelchair stability goes a long way in preventing injuries to the user. This requirement-while traversing a dynamic outdoor urban environment- is extremely important and there are a wide array of terrains that an autonomous wheelchair must handle and ensure stability for the user.
  - Examples:
    - Can not go back to pavement road from lawn surface.
    - Curb causing rolling over.
    - Cast wheels suspend the powered wheels, also it causes rolling over when one of the powered wheels touches ground first.
- This paper focuses on the challenge of traversing & mapping curbs



# Related Work/Curb Mapping

---

- General theory
  - SLAM
    - ORB-SLAM
    - RGBD/Stereo-SLAM
    - **We used:** graph-Slam (RTAB)
  - Mesh
    - Delaunay Triangulation
    - Alpha Shapes
    - **We used:** Poisson Reconstruction
- Applications to Wheelchairs
  - Different methods have been applied to outlined various information about the environment
    - One work focused on constructing a 3D safety map that outlined potential hazards



# Related Work/Stability Analysis

---

- There are two main categories of rollover
  - Tripped: Obstacle in environment causes configuration that leads to rollover
  - Untripped: Control behavior leads to rollover
- Development of dynamic models is extremely unique to each vehicle and dependent on assumptions
  - Suspension
  - Movement of center of mass
- We made 3 main assumptions...
  - The whole wheelchair is equivalent to rigid body
  - The wheelchair is symmetrical with the middle plane of the wheels on both sides, and the center of mass lies on the middle plane
  - The four-wheeled wheelchair model is equivalent to a two-wheeled model, where the two wheels in contact with the ground are equivalent to a longitudinal middle position, and the center of mass is located on this plane



# Curb Mapping

## 3D Mapping using SLAM

- RTAB (Real-Time Appearance-Based Mapping)
  - **Front-end:** *Periodically, the raw depth data and odometry is stored in a node that is connected to the other through vertices.*
  - **Back-end:** *This is where the graph is optimized to minimize the cost function for the graph and find the most likely configuration*
  - **Loop Closure:** *The loop closure detection algorithm employed using bag-of-words approach. Every time a node is created visual features are extracted and quantized to incremental visual vocabulary. Continually updating Bayes filter detects loop closures.*



# Curb Mapping

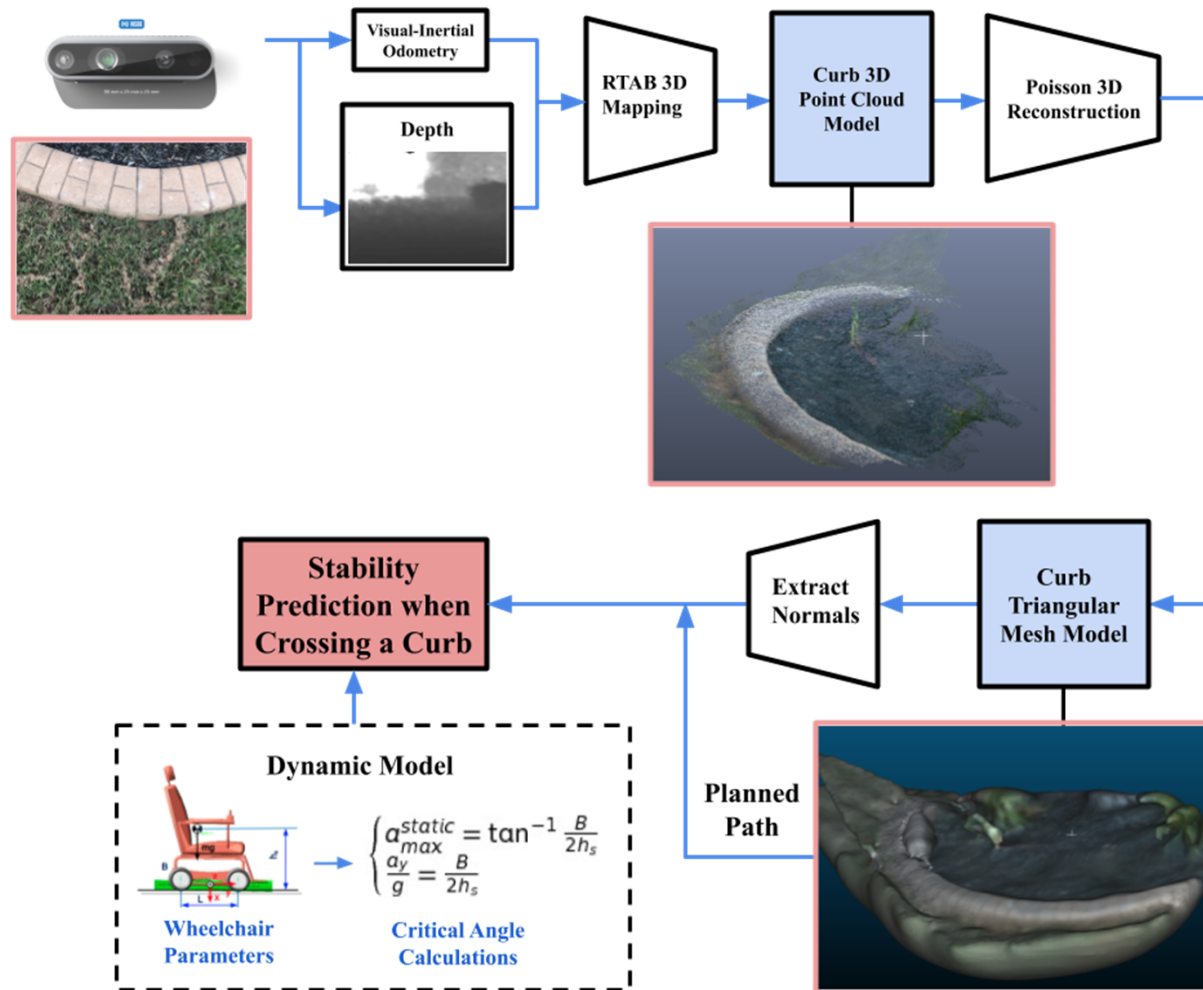
---

## 3D Mesh Generation

- Poisson reconstruction was used due to defining characteristic of resistance to data noise
- The goal of Poisson Reconstruction is to find an indicator function  $X$ , which defines an isosurface that represents the surface accurately
  - The gradient of the indicator function is equal to the vector field ( $\nabla(q)$ ) defined by the pointcloud
- Poisson Reconstruction has polynomial time in running so we subsampled the pointcloud to reduce the computation time



# Perception Pipeline Overview





# Dynamic Model for wheelchair

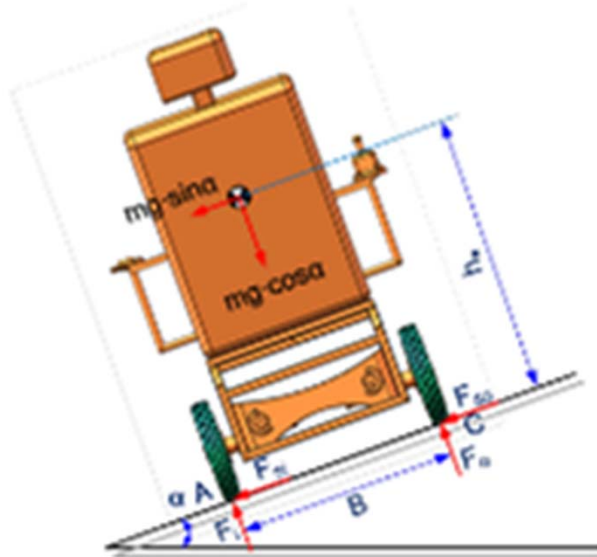


Fig. 2: Configuration of wheelchair in static rollover condition

$$\begin{cases} F_i + F_o &= mg \cos(\alpha) \\ F_{si} + F_{so} &= mg \sin(\alpha) \end{cases}$$

$$\begin{cases} F_1 &= \left(1 - \frac{B + (h_s \tan(\alpha) + \frac{B}{2})}{B}\right)mg \\ F_2 &= \frac{B - (h_s \tan(\alpha) + \frac{B}{2})}{B}mg \end{cases}$$

The above expressions were used to derive the terrain conditions for rollover in terms of the wheelchair.

## Static Rollover

- The slope of the terrain must make the net force about C equal to 0 ( $F_2 = 0$ )  
(Used to derive  $a_{\text{static}}$ )

$$a_{\text{max}}^{\text{static}} = \tan^{-1} \frac{B}{2h_s}$$

## Dynamic Rollover

- Similarly net force of wheelchair is supported by point A, meaning net force at point C is 0 ( $F_2 = 0$ ) (Used to solve for  $a_y/g$  Rollover indicator)
- Roll threshold value when the wheelchair is in a steady state condition which is used to evaluate the wheelchair's anti rollover capability.

$$\frac{a_y}{g} = \frac{B}{2h_s}$$



# Experiment

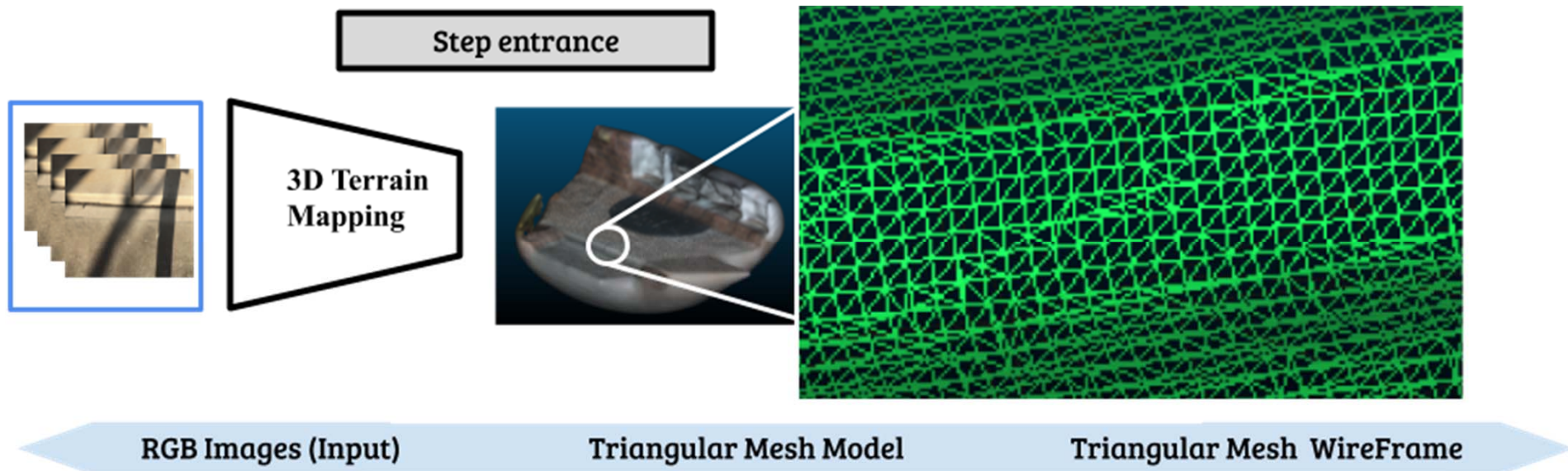
- **Setup/Field Data Collection**
  - The 3D mapping pipeline was run on an intel core i7, running Ubuntu 16.04 and ROS Kinetic
  - The terrains mapped fell into two categories: traversable and non-traversable
- **3D Mapping and Mesh Results**
  - ERMS (Edge Root Mean Square) was used to measure the quality of the produced mesh

$$ERMS_{\mu} = \frac{1}{N} \sum_{t \in \Lambda_t} \sqrt{\frac{t_{L1}^2 + t_{L2}^2 + t_{L3}^2}{3}}$$

| Edge Root Mean Square                     |         |         |          |         |
|---|---------|---------|----------|---------|
| K   | 0.5     | 0.7     | 0.9      | 0.97    |
| Poisson Reconstruction — $O(m^3 \log(m))$ |         |         |          |         |
| $\mu$                                     | 0.00665 | 0.00478 | 0.00413  | 0.00429 |
| $\sigma$                                  | 0.008   | 0.006   | 0.006    | 0.006   |
| Alpha Shapes — $O(m^2)$                   |         |         |          |         |
| $\mu$                                     | 0.01596 | 0.01398 | 0.01268  | 0.01232 |
| $\sigma$                                  | 0.014   | 0.013   | 0.012    | 0.012   |
| Delaunay Triangulation — $O(m \log(m))$   |         |         |          |         |
| $\mu$                                     | 0.02621 | 0.02498 | 0.024193 | 0.02394 |
| $\sigma$                                  | 0.057   | 0.057   | 0.057    | 0.057   |

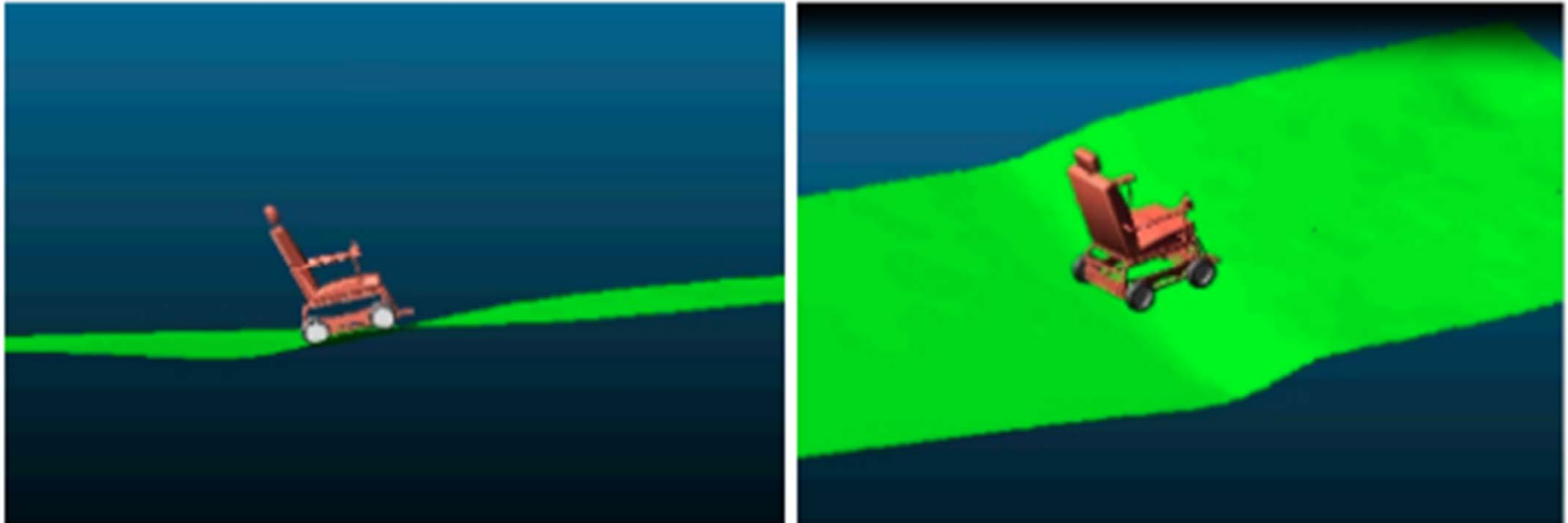


# Mesh Generation Visualization





# Dynamic Simulation on Field Collected Data in ADAMS



## Wheelchair Specifications:

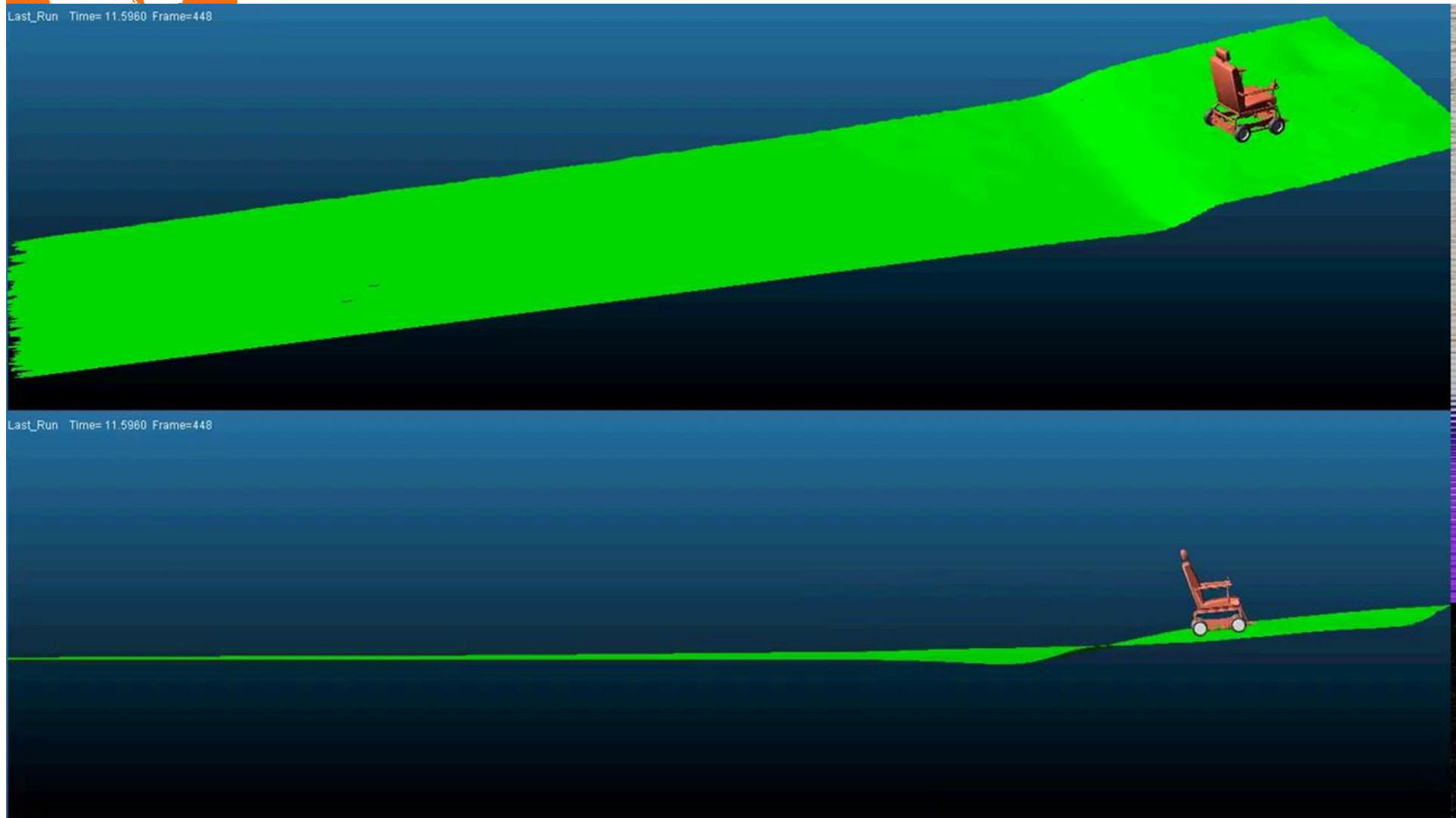
- Three-dimensional size of the wheelchair (length x width x height) is \$1000 x 710mm x 1320mm\$
- The wheelbase B is 650mm
- The wheelbase L is 575mm
- Wheelchair's distance to the mass centroid from the ground \$h\_s\$ is 451mm
- Mass 165 kg

## Terrain Specifications:

- Main obstacle: curb
- “.rdf” format

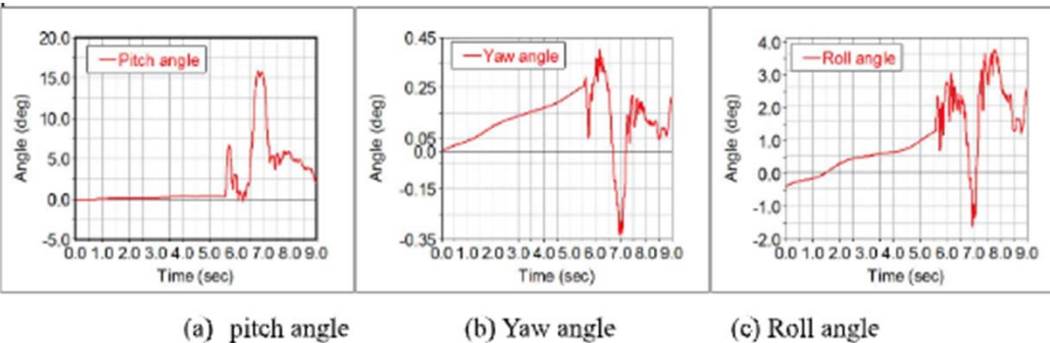


# Demonstration





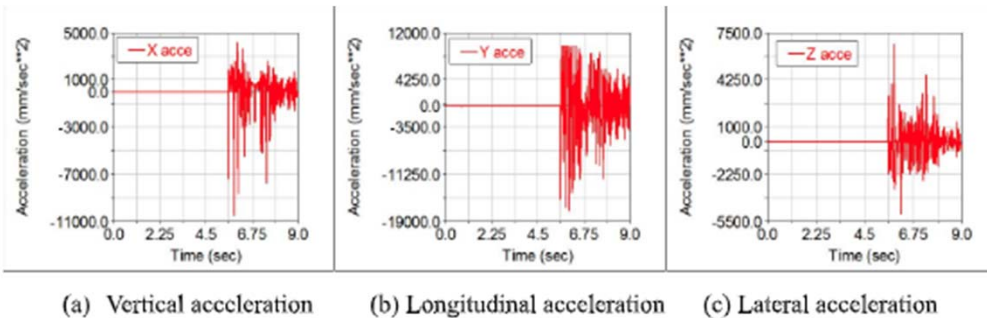
# Dynamic Simulation on Field Collected Data Results



(a) pitch angle

(b) Yaw angle

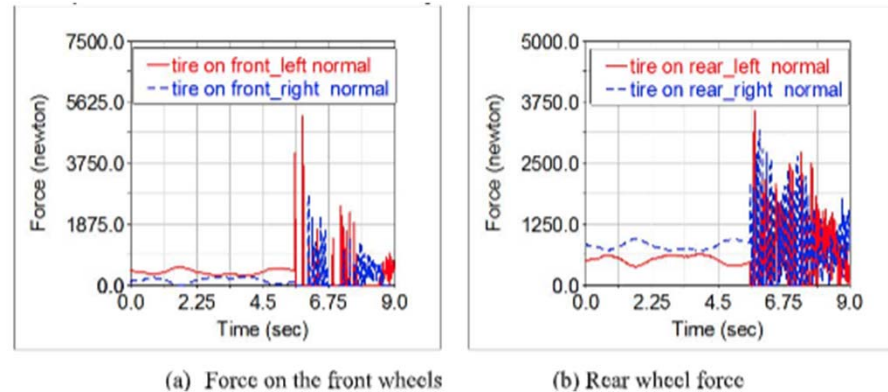
(c) Roll angle



(a) Vertical acceleration

(b) Longitudinal acceleration

(c) Lateral acceleration



(a) Force on the front wheels

(b) Rear wheel force

**Posture Angle:** The range of the angle is only (-1.6 degrees, 3.7 degree), which provides intuitive data prediction for anti-rollover control.

**Curve of Acceleration:** The maximum roll acceleration of the wheelchair is about 0.6g, which is used to predict the rollover state of the wheelchair

**Normal Forces:** Force of the four wheels on the flat road is relatively uniform, and the normal force fluctuates between 400N-500N. When the wheelchair is driving on the rough road and crossing the curb, the four wheels are unevenly stressed and bumps occur



# Dynamic Simulation Unstable Configs



(a) Lateral sliding



(b) Roll over

The unstable configuration of the wheelchair falls in two categories: lateral sliding & rollover. Which one it falls into depends on coefficient of friction.



## Future Works

---

- Integrate more terra mechanical properties of curbs than simply gradient into stability prediction for wheelchair.
- Apply pipeline to a real-world wheelchair and refine dynamic model
- Occupant centered stability



# Citations

---

1. Matthew Bolitho, Michael Kazhdan, Randal Burns, and Hugues Hoppe. Parallelpoisson surface reconstruction.Advances in Visual Computing Lecture Notes inComputer Science, page 678–689, 2009.
2. Jorge Candiotti, S. Andrea Sundaram, Brandon Daveler, Benjamin Gebrosky, Gar-rett Grindle, Hongwu Wang, and Rory A. Cooper. Kinematics and stability analysisof a novel power wheelchair when traversing architectural barriers.Topics in SpinalCord Injury Rehabilitation, 23(2):110–119, 2017.
3. Alicia M et al. Koontz. Wheeled mobility.BioMed research international, 2015.
4. M. Levesley, S. Kember, David Barton, P. Brooks, and Osvaldo Querin. Dynamicsimulation of vehicle suspension systems for durability analysis.Materials ScienceForum - MATER SCI FORUM, 440-441:103–110, 01 2003.
5. A. Murarka, J. Modayil, and B. Kuipers. Building local safety maps for a wheelchairrobot using vision and lasers.The 3rd Canadian Conference on Computer and RobotVision (CRV06).
6. Brad Schofield, Tore Hagglund, and Anders Rantzer. Vehicle dynamics control andcontroller allocation for rollover prevention.2006 IEEE International Conferenceon Control Applications, 2006.
7. Cheng Zhao, Huosheng Hu, and Dongbing Gu. Building a grid-point cloud-semanticmap based on graph for the navigation of intelligent wheelchair.2015 21st Interna-tional Conference on Automation and Computing (ICAC), 2015